Appl. Phys. B 76, 815–819 (2003)
DOI: 10.1007/s00340-003-1228-1

Applied Physics B
Lasers and Optics

B. SMEETS[1,✉]
R.C.M. BOSCH[1]
P. VAN DER STRATEN[1]
E. TE SLIGTE[1]
R.E. SCHOLTEN[2]
H.C.W. BEIJERINCK[1]
K.A.H. VAN LEEUWEN[1]

Laser frequency stabilization using an Fe-Ar hollow cathode discharge cell

[1] Eindhoven University of Technology, Department of Physics, P.O. Box 513, 5600MB Eindhoven, The Netherlands
[2] School of Physics, University of Melbourne, Victoria 3010, Australia

Received: 14 February 2003/Revised version: 16 May 2003
Published online: 9 July 2003 •

ABSTRACT Polarization spectroscopy of an Fe-Ar hollow cathode discharge cell was used to lock a frequency-doubled Ti:sapphire laser to the 372-nm $^5D_4 \rightarrow {}^5F_5$ transition of ^{56}Fe. The discharge cell produced a density of 10^{18} m^{-3} ground-state ^{56}Fe atoms at a temperature of 650 K, this density being comparable to a conventional oven at 1500 K. Saturated absorption spectroscopy and two schemes of polarization spectroscopy were compared with respect to signal-to-background ratio and the effect of velocity-changing collisions. The laser was locked within 0.2 MHz for hours by feedback of the dispersive polarization spectroscopy signal.

PACS 33.55.Ad; 42.62.Fi; 52.25.Ya

1 Introduction

Atom optics experiments often require the ability to lock lasers to the frequency of an atomic transition within an atomic line width. To achieve this, a high-resolution spectroscopic technique is needed.

In our group, we are investigating direct-write atom lithography of Fe [1]. This technique has been applied successfully to sodium [2, 3], chromium [4–7] and aluminum [8] beams. It has proven to be a very promising technique for the production of regular arrays of nanostructures. In this approach an atomic beam is focused by the interaction with a high-intensity, near-resonant standing wave. In our experiment, a supersonic Fe atom beam will be used to reduce 'monochromatic aberrations' during focusing [9]. Spherical aberration is reduced by collimating the Fe beam to a divergence of 100 μrad by laser-cooling techniques [10].

The only atomic transition of ^{56}Fe that can be used for laser focusing and cooling is the $^5D_4 \rightarrow {}^5F_5$ transition, which corresponds to an optical wavelength of 372.099 nm in vacuum [11]. No commercial laser is available at this wavelength with the power needed to focus and collimate the Fe atoms, approximately 500 mW. To meet these specifications, we use a commercially available titanium sapphire (Ti:S) laser, frequency doubled with an LBO crystal placed inside a resonant ring cavity. A schematic of the laser setup is shown in Fig. 1.

✉ Fax: +31-40/245-6050, E-mail: b.smeets@tue.nl

In most atom optics experiments, the laser is locked to the atomic transition by using spectroscopy in a vapor cell or an atomic beam. In vapor cells, two Doppler-free spectroscopy schemes are most popular for locking lasers to atomic transitions. One is based on saturated absorption spectroscopy [12], which creates a dispersive locking signal by dithering the laser frequency or the transition frequency. The laser frequency is dithered with an electro-optical (EO) or acousto-optical (AO) modulator in the laser beam, the transition frequency is dithered by a modulated magnetic field over the cell. The other Doppler-free locking scheme is based on polarization spectroscopy [12], which creates a dispersive locking signal without use of frequency modulators.

This paper describes the use of polarization spectroscopy in an Fe-Ar hollow cathode discharge cell (Sect. 2). The cell and its discharge properties are discussed (Sect. 3). Signal-to-background levels of polarization spectroscopy and saturated absorption spectroscopy are investigated, and two different schemes of polarization spectroscopy are used to investigate the effects of velocity-changing collisions (VCCs) in the polarization spectroscopy signals. The isotope shift for ^{54}Fe and the frequency offset of one of the hyperfine components for

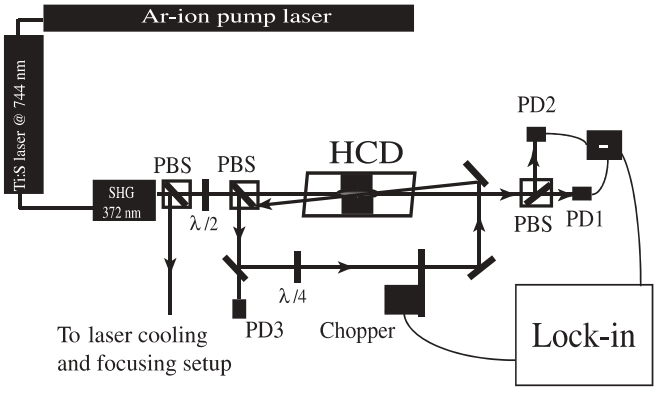

FIGURE 1 Experimental arrangement: an Ar-ion laser (Coherent Innova 200) pumped a Ti:S laser (Coherent 899-21), which was frequency doubled with a LBO crystal inside a ring cavity. Part of the doubled beam was used for spectroscopy. Probe and pump beams were split with a polarizing beam splitter (PBS), which in combination with a $\lambda/2$ wave plate also balanced the intensities. The beams were counter-propagating through the hollow-cathode discharge. The probe beam was analyzed by one or two photodiodes (PD1 and PD2) and a lock-in amplifier referenced to the chopped pump beam. The laser power before absorption was measured by PD3

the ^{57}Fe frequency shift are measured (Sect. 4). By integration of the dispersive-shaped signal, the laser is locked on the $^5D_4 \rightarrow {}^5F_5$ transition of ^{56}Fe.

2 Hollow cathode discharge cell

In a regular vapor cell, producing sufficient Fe requires a temperature in the order of 1500 K. As an alternative, we used a hollow cathode discharge cell, in which a high vapor pressure can be reached at lower temperature by sputtering. They are commonly used to perform high-resolution spectroscopy of metal vapors [13–15]. See-through hollow-cathode discharges are commercially available [16]. However, we followed the design of a Cr hollow-cathode discharge of Mlynek's group at the University of Konstanz [5, 7] (Fig. 2).

The cell consisted of an Fe hollow cathode with a length of 20 mm and an inner diameter of 5 mm. Two stainless steel anode rings were mounted at 5 mm from the ends of the hollow cathode to maintain a uniform discharge. The cathode was placed between two pyrex half-tubes, which carried the connectors for the anodes and Ar feed-through. The pyrex tubes were clamped to the cathode block and sealed with o-rings. A continuous flow of Ar was applied to keep the cell clean. The pressure in the cell could be varied from approximately 1 to 2 Torr. The cathode was cooled with water at 17 °C.

The discharge current was provided by two 300-V, 100-mA current-stabilized power supplies in parallel. The cathode current was adjusted between 40 mA and 200 mA, for discharge voltages of 260 V to 280 V, at both 1- and 2-Torr Ar pressure.

3 Absorption spectroscopy

Doppler-limited absorption spectroscopy was used to determine the temperature and density of the Fe atoms in the discharge.

At thermal equilibrium, the atoms in the gas cell should follow a Maxwellian velocity distribution. At a temperature T the corresponding Doppler line-shape function is given by [17]

$$S(\nu) = \frac{c}{\nu_0}\left(\frac{m}{2\pi kT}\right)^{1/2} \exp\left(\frac{-mc^2(\nu-\nu_0)^2}{2kT\nu_0^2}\right), \quad (1)$$

with m the mass of the atoms and ν the frequency of the light, ν_0 the resonance frequency, k the Boltzmann constant, and c the speed of light. The absorption of light by the atoms in the cell can be described by the Beer–Lambert relation:

$$I/I_0 = \exp(-aL), \quad (2)$$

with I_0 and I the intensity of the incident and transmitted light. The parameter a is the absorption coefficient and L is the interaction length. On resonance the absorption coefficient is

$$a(\nu_0) = n\sigma(\nu_0), \quad (3)$$

with $\sigma(\nu_0)$ the absorption cross section on resonance and n the density of the ground-state Fe atoms. The semi-classical expression for the absorption cross section on resonance is

$$\sigma = \frac{3}{4}\lambda^2 C_A^2 \Gamma S(\nu_0), \quad (4)$$

with λ the wavelength of the atomic transition, $C_A^2 = 0.407$ the weighted average over the relevant Clebsch–Gordan coefficients, and Γ the natural line width 2.58 MHz [11] of the $^5D_4 \rightarrow {}^5F_5$ transition of Fe. The ground-state density can therefore be determined from the intensity ratio of the laser before and after the gas cell and the Doppler line profile on resonance.

To measure the absorption by the Fe atoms the Ti:S laser was scanned over a 4-GHz range, which corresponds to 8 GHz in the UV. Frequency calibration was performed using a Fabry–Pérot etalon (FSR $= 150.0 \pm 0.5$ MHz at 744 nm). The intensity of the laser beam was approximately 0.25 times the saturation intensity of 62 μW/mm^2. The laser-beam diameter was approximately 1 mm. The laser intensity before and after the gas cell was measured by PD3 and PD1, respectively (Fig. 1).

Density and temperature of ground-state Fe atoms were measured at three different radial positions and at 1- and 2-Torr Ar pressure. The position range was limited by the size of the laser beam and the hollow cathode inner diameter. The pressure range was limited by the design of the gas inlet system and the discharge current.

The data in Fig. 3 show the temperature of the Fe ground-state atoms as a function of the discharge current at three radial positions for 1- and 2-Torr Ar pressure. The statistical uncertainty in the temperature is ± 30 K. No significant difference is observed between the temperatures at different radial positions. The large fluctuations at 40 mA were due to instabilities in the discharge. At 2-Torr Ar pressure, the Fe discharge was not stable below 120 mA. Note that the lower temperatures at 2 Torr were due to the larger heat conductivity by the Ar atoms.

Figure 4 shows the column density (integrated density times length) as a function of radial position. The statistical uncertainty in the data points is 10^{15} m^{-2}, determined

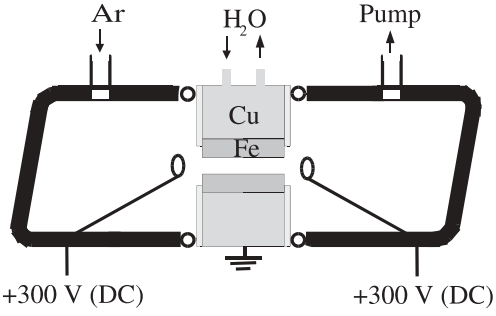

FIGURE 2 Scheme of the hollow cathode discharge cell. The cell consisted of a Fe hollow cathode with a length of 20 mm and an inner diameter of 5 mm. Two stainless steel anode (300 V) rings were mounted, at approximately 5 mm from the ends of the hollow cathode, to maintain a uniform discharge. The cathode was placed between two pyrex half-tubes, which carried the connectors for the anodes and Ar feed-through. The cell was sealed with Viton o-rings. The pressure in the cell could be varied from approximately 1 to 2 Torr. The cathode was grounded and cooled with water at 17 °C

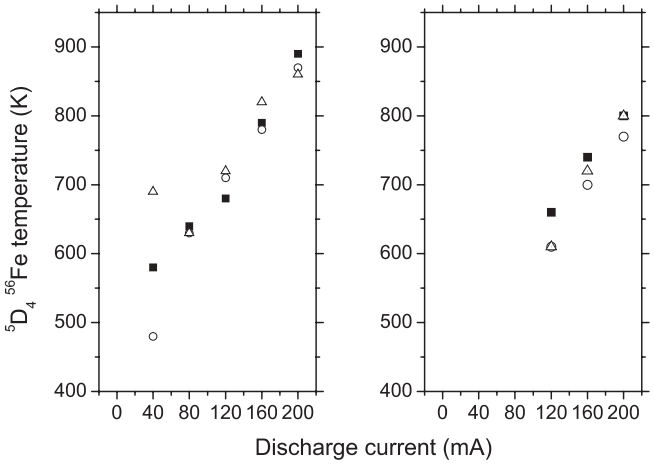

FIGURE 3 Temperature of ground-state Fe atoms as function of cathode current for 1-Torr (*left*) and 2-Torr (*right*) Ar pressure at three different radial positions: center of cathode (*closed boxes*), 0.75 mm from center (*open circles*), and 1.5 mm from center (*open triangles*)

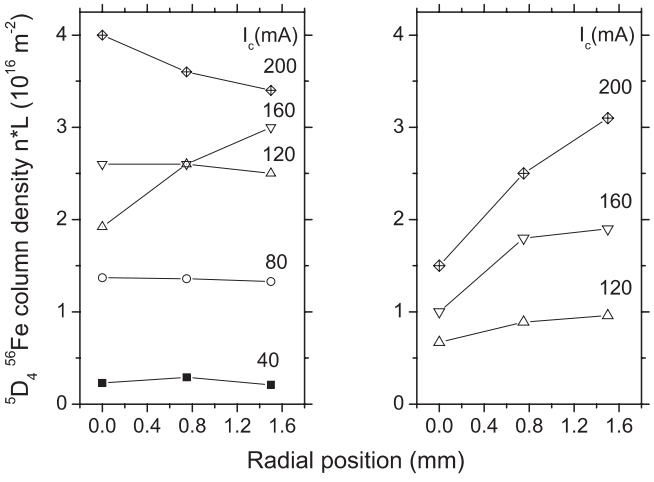

FIGURE 4 Column density as a function of radial position for 1-Torr (*left*) and 2-Torr (*right*) Ar pressure at different cathode currents I_c

from repeated measurements. Assuming for the sake of simplicity a uniform density along the discharge and an effective length equal to the hollow-cathode length ($L = 20$ mm), densities were in the order of 10^{18} m^{-3} (10^{-4} Torr) and temperatures around 650 K. An equivalent thermal vapor cell would require a temperature of 1500 K to achieve a similar density. The effect of saturation by the laser light has not been taken into account in the density measurements. A saturation parameter of 0.25 implies approximately 5 percent less total absorption compared to zero incident laser power. The measured density is thus 5 percent lower than the actual density in the cell, which is within the statistical uncertainty.

It is expected that, at higher Ar pressures, the Fe density in the middle of the hollow cathode will decrease due to better charge transfer between Fe atoms and Ar ions [18]. Comparing the corresponding 1-Torr and 2-Torr data of Fig. 4, the density was significantly lower in the center of the hollow cathode at 2-Torr Ar pressure. No clear systematic deviations from a homogeneous density were observed at 1 Torr.

4 Laser locking by polarization spectroscopy

The basic theory of polarization spectroscopy (PS) can be found in [12]. Two laser beams, a linearly polarized probe beam and a circularly polarized pump beam, are counter-propagating inside the gas cell. The polarization of the probe beam becomes slightly elliptical, with the main axis of the ellipse slightly rotated with respect to the initial polarization direction because of the non-uniform distribution of magnetic sublevels of the Fe atoms in the discharge due to the circularly polarized pump beam. The probe beam is analyzed by a polarizing beam-splitter cube (PBS), of which the principal axis is at 45 or 90 degrees with respect to the polarization of the probe beam. If the cube is at 90 degrees with the probe-beam polarization, a non-dispersive signal is observed that is a measure of the change in polarization. With the PBS principal axis at 45 degrees, a dispersive signal can be extracted by subtracting the signals of the light reflected and transmitted by the PBS.

In contrast with saturated absorption spectroscopy, polarization spectroscopy can thus provide a dispersive locking signal without the use of frequency modulation and phase-sensitive detection. However, the measured signals are small and detection noise becomes important. To separate the pure polarization spectroscopy signal from the Doppler-broadened background, the pump beam was chopped at 2 kHz and a lock-in amplifier was used (Fig. 1).

Another advantage of polarization spectroscopy over saturated absorption spectroscopy should be the improved signal-to-background ratio, as the background signal is largely reduced by the use of the PBS and only the change in polarization is observed.

To compare the signal-to-background level of both techniques, we measured both the saturated absorption signal, using a linear polarized probe and a linear polarized chopped pump beam, and the polarization spectroscopy signal with the same set of detectors. Figure 5 shows the polarization spectroscopy and saturated absorption spectroscopy signals, with and without the use of a lock-in amplifier. The sensitivity of polarization spectroscopy is mainly limited by the detection noise. The ratio between signal and off-resonance background is much larger for polarization spectroscopy than for saturated absorption spectroscopy. However, because of the small absolute value of the polarization spectroscopy signal, detection noise becomes significant. The lock-in signals of both spectroscopic techniques therefore display a comparable signal-to-noise level. Polarization spectroscopy without a lock-in amplifier would only be advisable when low-noise detectors are used. Both the polarization and saturated absorption signals suffer from a Doppler pedestal, which is due to velocity-changing collisions (VCCs). During interaction with the two laser beams, the velocity of the atoms is redistributed by collisions such that the interaction of light with those atoms contributed to the signal at other frequencies.

To overcome the problem of VCCs, another polarization spectroscopy scheme was used [19], which is known to be pedestal-free. In this scheme, the probe beam is circularly polarized and the pump beam linearly polarized by placing a $\lambda/4$ wave plate in the probe beam. With the PBS at 90 degrees the non-dispersive laser-induced dichroism signal was measured

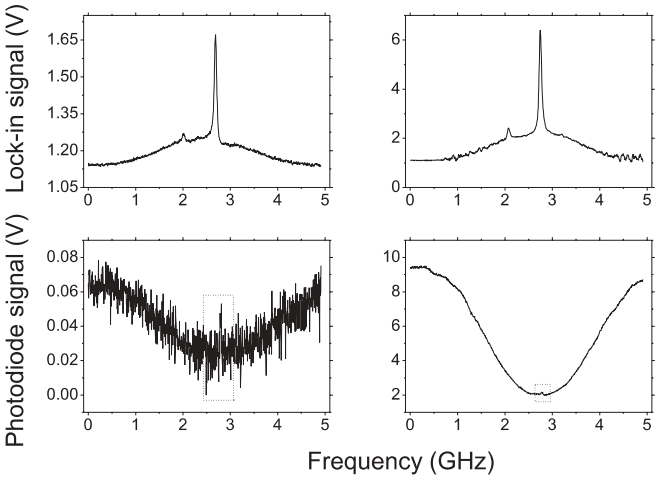

FIGURE 5 Comparison between polarization spectroscopy (*left*) and saturation spectroscopy (*right*), measured with (*top*) and without (*bottom*) a lock-in amplifier. The *boxes* indicate the Doppler-free polarization and saturated absorption signals. The signal-to-background level for polarization spectroscopy is large compared to saturated absorption spectroscopy. However, the polarization spectroscopy signal is so small that the signal-to-noise levels for both techniques are comparable

(Fig. 6, left). Because of the circular probe, the signals of the transmitted and reflected light from the PBS had to be subtracted. Rotating the PBS to 45 degrees gave the dispersive laser-induced birefringence signal (Fig. 6, right).

The birefringence signals from both schemes are shown in Fig. 7. The appearance of a Doppler pedestal when velocity-changing collisions are present indicates that the anisotropy in magnetic sublevels induced by the pump beam can survive collisions. With a circularly polarized pump beam, the atoms are pumped to the extreme magnetic sublevels ($M = -J$ or $M = J$). Assuming that a collision with an Ar atom cannot induce a large change in orientation of a Fe atom, the Fe atoms will remain partly polarized and the medium will remain anisotropic. In contrast, with a linear pump beam an incomplete transfer to the low-M sublevels will be accomplished. It appears that this anisotropy is less robust against collisions with Ar atoms.

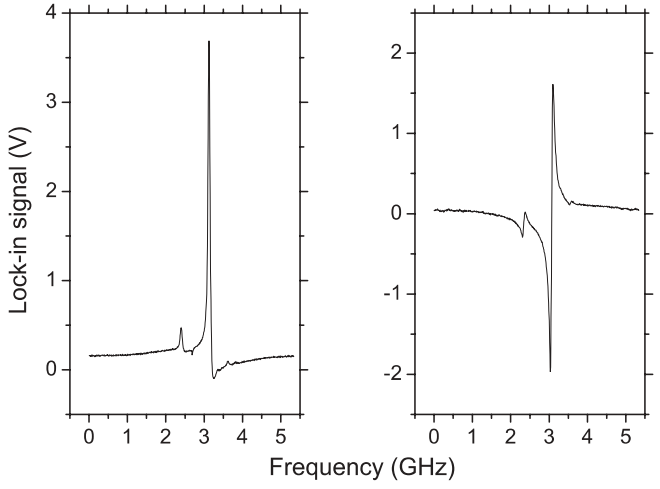

FIGURE 6 Laser-induced dichroism (*left*) and laser-induced birefringence (*right*) signals. The slight dispersive shape of the dichroism signal is due to a small misalignment of the PBS

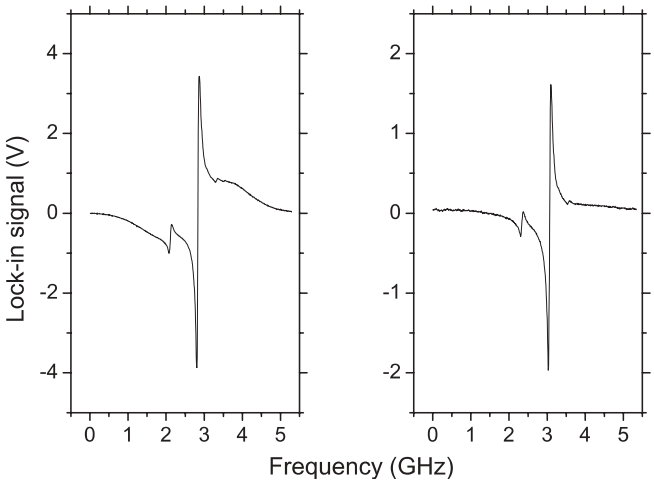

FIGURE 7 *Left*: birefringence signal of the polarization spectroscopy scheme with circular pump. *Right*: birefringence signal of the polarization spectroscopy scheme with circular probe

The minimal measured width of the Doppler-free signals was 33 ± 3 MHz. Attempts were made to reduce this width. Using a beam splitter to reflect the pump beam into the discharge cell, the offset angle between pump and probe beams was nominally reduced to zero. However, the width was not significantly reduced. No significant broadening of the signals could be measured between 1 and 2-Torr Ar pressure, so pressure broadening cannot explain the width of the signals. Another broadening effect in hollow-cathode discharges is Stark broadening, due to transient electric field variations in the discharge. Also, the presence of non-uniform magnetic fields in our ferromagnetic hollow-cathode discharge could broaden the signals significantly. Power broadening, wavefront imperfections in the beams, and very small angle elastic collisions are small effects, which would broaden the signals in the order of 5 MHz.

In the signals of Figs. 6 or 7, the contributions of other isotopes of Fe are visible. The element Fe has four stable isotopes, with natural abundances of 5.8 percent ^{54}Fe, 91.8 percent ^{56}Fe, 2.1 percent ^{57}Fe, and 0.3 percent ^{58}Fe. The smaller signal below resonance was, considering the natural abundances, the contribution of ^{54}Fe. The corresponding measured isotope shift is -725 ± 10 MHz with respect to the ^{56}Fe transition. The tiny signal above resonance is a contribution from ^{57}Fe, with a corresponding measured shift of 495 ± 10 MHz with respect to the ^{56}Fe transition. Isotope ^{57}Fe has nuclear spin of $I = 1/2$; thus, this isotope is a fermion with the hyperfine structure of ground and excited levels ($F = 7/2, 9/2$) and ($F = 9/2, 11/2$), respectively. Five contributions of ^{57}Fe should be present in the signal, including two cross-over resonances. Only one component was observed: the other contributions were either too small or they overlapped with the other dispersive signals. To measure the isotope shift of ^{57}Fe the shifts of all components should be measured. The contribution from ^{58}Fe was too small to measure.

The laser was locked on the zero crossing of the dispersive signal by integration-only feedback to the laser external frequency control input. In both polarization spectroscopy schemes the frequency of the laser can be tuned by optical or electronic means. By changing the polarization of the probe

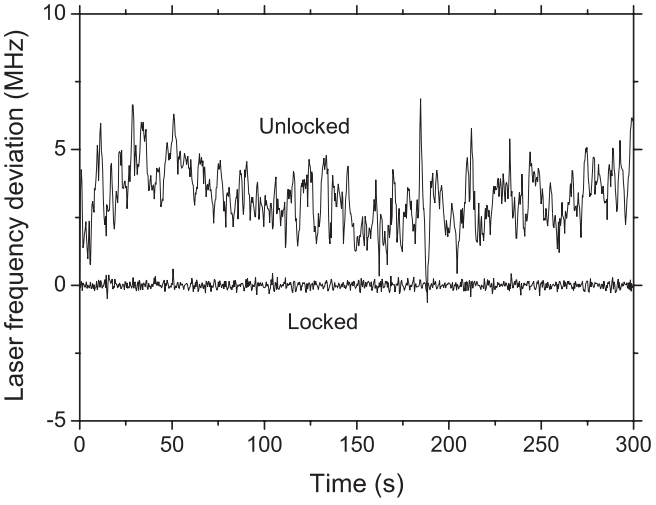

FIGURE 8 The effect of the locking circuit on the long-term stability of the laser frequency. The locking point was chosen on the zero crossing of the dispersive signal

beam an imbalance in the two polarization components of the probe beam can be induced, which shifts the dispersive signal up or down and thus shifts the zero-crossing point. Electronically, the frequency can be detuned by applying an offset on the integrator. We have used the latter technique. The laser stability was determined by measuring the amplitude of the dispersive error signal, which was related to the frequency deviation with a previous calibration frequency scan. We measured the amplitude of the dispersive error signal obtained with a circularly polarized pump beam to be larger than that with a linearly polarized pump beam, which is favorable for locking. Figure 8 shows the effect of locking on the laser frequency by measuring the amplitude of the dispersive signal as a function of time. Typically, the laser lock was stable within 0.2 MHz for hours.

5 Conclusions

We have built an Fe-Ar hollow cathode discharge cell to lock a frequency-doubled Ti:S laser to the 372-nm $^5D_4 \rightarrow {}^5F_5$ transition of ^{56}Fe by means of polarization spectroscopy. Ground-state densities in the order of 10^{18} m^{-3} were reached with temperatures of 600 to 700 K. In a standard oven, 1500 K would be necessary to reach a comparable density. Both polarization and saturated absorption spectroscopy showed comparable signal-to-noise levels. The signal-to-noise level of polarization spectroscopy is limited by detection noise. In the polarization spectroscopy scheme with circular pump and linear probe a Doppler pedestal induced by velocity-changing collisions remained present. To overcome this problem, we used a scheme with a circular probe beam and a linear pump beam. The minimal measured Doppler-free width was 33 ± 3 MHz. Two signals from other Fe isotopes were measured. The signal corresponding to the ^{54}Fe isotope was shifted by -725 ± 10 MHz with respect to the ^{56}Fe transition frequency. The contribution of one of the hyperfine transitions of ^{57}Fe was shifted by 495 ± 10 MHz with respect to the ^{56}Fe transition frequency. The laser was locked by integrating the dispersive signal. The laser remained locked well within 0.2 MHz for hours.

ACKNOWLEDGEMENTS This work is financially supported by the Dutch Foundation for Fundamental Research on Matter (FOM).

REFERENCES

1 E. te Sligte, R.C.M. Bosch, B. Smeets, P. van der Straten, H.C.W. Beijerinck, K.A.H. van Leeuwen: Proc. Natl. Acad. Sci. **99**, 6509 (2002)
2 V. Natarajan, R.E. Behringer, G. Timp: Phys. Rev. A **53**, 4381 (1996)
3 G. Timp, R.E. Behringer, D.M. Tennant, J.E. Cunningham: Phys. Rev. Lett. **69**, 1636 (1992)
4 J.J. McClelland, R.E. Scholten, E.C. Palm, R.J. Celotta: Science **262**, 877 (1993)
5 U. Drodofsky, J. Stuhler, B. Brezger, Th. Schulze, M. Drewsen, T. Pfau, J. Mlynek: Microelectron. Eng. **35**, 285 (1997)
6 R. Gupta, J.J. McClelland, Z.J. Jabbour, R.J. Celotta: Appl. Phys. Lett. **67**, 1378 (1995)
7 U. Drodofsky, J. Stuhler, Th. Schulze, M. Drewsen, B. Brezger, T. Pfau, J. Mlynek: Appl. Phys. B: Photophys. Laser Chem. **65**, 755 (1997)
8 R.W. McGowan, D.M. Giltner, S.A. Lee: Opt. Lett. **20**, 2535 (1995)
9 R.C.M. Bosch, H.C.W. Beijerinck, P. van der Straten, K.A.H. van Leeuwen: Eur. Phys. J.: Appl. Phys. **18**, 221 (2002)
10 R.E. Scholten, R. Gupta, J.J. McClelland, R. Celotta, M.S. Levenson, M.G. Vangel: Phys. Rev. A **55**, 1331 (1997)
11 H.M. Crosswhite: J. Res. Natl. Bur. Stand. (USA) **79A**, 17 (1975)
12 W. Demtröder: *Laser Spectroscopy* (Springer, Berlin 1981) p. 505
13 Ph. Dabkiewicz, T.W. Hansch: Opt. Commun. **38**, 351 (1981)
14 S. Kroll, A. Persson: Opt. Commun. **54**, 277 (1985)
15 L. Gianfrani, O. Monda, A. Sasso, M.I. Schisano, G.M. Tino, M. Inguscio: Opt. Commun. **83**, 300 (1991)
16 Cathodeon Ltd.: http:\\www.cathodeon.com; Hamamatsu: http:\\www.hamamatsu.com
17 P.W. Milonni, J.H. Eberly: *Lasers* (Wiley, New York 1988) pp. 101–111
18 B.E. Warner, K.B. Persson, G.J. Collins: J. Appl. Phys. **50**, 5694 (1979)
19 C. Delsart, J.C. Keller: 'Doppler-Free Laser Induced Dichroism and Birefringence'. In: Laser Spectroscopy III, Proc. 3rd Int. Conf., Jackson Lake, 1977 (Springer Ser. Opt. Sci. **7**) (Springer, Berlin 1977) p. 154